

# CHEIA ANTENNAS RETROFIT TO A SPACE TRACKING RADAR

Dr. Liviu Ionescu<sup>(1)</sup>, Roberto Scagnoli<sup>(2)</sup>, Dan Istriteanu<sup>(3)</sup>, Dr. Vlad Turcu<sup>(4)</sup>

<sup>(1)</sup>Rartel SA, Str. Iacob Felix nr. 70, Sector 1, Bucharest, Romania, Email: [liviu.ionescu@rartel.ro](mailto:liviu.ionescu@rartel.ro)

<sup>(2)</sup>Rartel SA, Str. Iacob Felix nr. 70, Sector 1, Bucharest, Romania, Email: [roberto.scagnoli@rartel.ro](mailto:roberto.scagnoli@rartel.ro)

<sup>(3)</sup>Rartel SA, Str. Iacob Felix nr. 70, Sector 1, Bucharest, Romania, Email: [dan.istriteanu@rartel.ro](mailto:dan.istriteanu@rartel.ro)

<sup>(4)</sup>Romanian Academy, Cluj-Napoca Branch, Astronomical Observatory Cluj, Email: [vladturcu@yahoo.com](mailto:vladturcu@yahoo.com)

## ABSTRACT

Inaugurated in October 1976, the Cheia Satellite Communication Center from Prahova County, Romania, was the biggest teleport in the Central and South-Eastern Europe, comprising two 32m Intelsat Standard A high performance antennas, formerly used for international telephony. Due to the massive development of optical fiber links, the antennas were decommissioned, even though the site still offers other type of satellite communication services. The decommissioned antennas are an expensive piece of equipment that could be used for another type of services. This paper describes the intended retrofit of the Cheia 32m antennas into a LEOs tracking radar.

## 1. INTRODUCTION

Inaugurated in October 1976, the Cheia Satellite Communication Center from Prahova County, Romania, was the biggest teleport in the Central and South-Eastern Europe.

Due to its position, at the edge of the coverage area of the Intelsat satellite network over the Atlantic Ocean, the transmission parameters at that time required high power and very good reception sensitivity which resulted in a very performing 32 m dish antenna.

In 1979, a second similar antenna covering the Indian Ocean area was added to the site making the Cheia Satellite Communication Center the most important voice and data gateway in the region.

The Cheia site comprises 2 decommissioned 32m diameter parabolic antennas positioned at Latitude 45°27'24" N and Longitude 25°56'48" E. The site altitude is 900 m. Each antenna is mounted on top of its own support building.

The antennas baseline encompass 80 m, and its localization with respect to geographical coordinates is about 7° Azimuth from North, a roughly NNE – SSW orientation.

Besides the two 32 m antennas the site comprises several smaller antennas used for specialized satellite services, a communication tower, one technical equipment building and one administrative building as showed in Fig. 1.



Figure 1. Cheia site and antennas (Google Earth)

## 2. SITE'S EQUIPMENT AND CONSTRAINTS

### 2.1 Two almost identical high gain antennas

For the purpose of the retrofit as space radar, the Cheia site's main assets are the two 105-feet (32 m) diameter class, Cassegrain beam-waveguide antennas designed, manufactured and installed by Nippon Electric Co., Ltd (NEC), Tokyo, Japan in 1976 and 1979 respectively. Taking into account that the antenna system represents a significant portion of space radar's implementation costs, the presence of the two decommissioned antennas is one of the main reasons for this retrofit.

The antennas are almost identical, each of them providing the following functionalities:

- monopulse autotracking for satellite beacon signals in the 4 GHz band;
- transmission and reception of dual circular polarized signals in the 6 GHz and 4 GHz bands respectively.

The shaped Cassegrain antenna system is composed of a main reflector and a subreflector whose special shapes are computer calculated and based on experimental data of the 4-Reflector Primary Feed for the maximization of the figure of merit (G/T ratio). The aperture (D) of the main reflector and the focal length of its associated paraboloid are designed to provide the maximum gain while satisfying the structural requirements. If costs are to be kept in control, it is not advisable to alter the antenna or the antenna feeder system.

The most important parameters of the antennas are presented in Table 1:

Table 1 Main Antenna parameters

Nr.	Parameter	Cheia 1	Cheia 2
1	Effective gain at feed	>64dB	>63,9dB
2	First side lobe	-14 dB	
3	Sidelobes ( $1^{\circ}$ - $48^{\circ}$ )	32-25Log $\theta$	
4	Sidelobes ( $>48^{\circ}$ )	- 10 dB	
5	Noise temperature $\epsilon=20^{\circ}$	37,0	36,5
6	Noise temperature $\epsilon=30^{\circ}$	34,0	34,1
7	Bandwidth	3,6-6,4 GHz	
8	Isolation between antennas sidelobes	>93 dB	
9	Polarization	Dual circular	
10	Polarization isolation	30 dB	
	Total weight	309 ton	260 ton
11	Azimuth scanning domain	-170° to +170° relative S	
12	Elevation scanning domain	0°-92°	
13	Tracking speed	0,3°/s	0,3°/s
14	Deicing	Electrical	Electrical

The presence of two functional antennas allows the implementation of Continuous Wave (CW) radar designed to use both antennas, or pulsed radar designed to use only one antenna. A hybrid solution of CW/Pulsed radar using both antennas might be designed as well.

### 2.2 Antenna-feeder system power limitation

The antenna power handling capability in the 6GHz band, by using the existing structure of the composite feed is 10kW CW maximum.

The simulations performed for a 2,5kW CW power show acceptable size of the observed space objects. Detection and tracking can be performed on LEOs at 2000 Km altitude with size over 40cm. In the case of pulsed radar with a duty cycle of 30% the size is 3 times larger.

### 2.3 Antenna-feeder system bandwidth

The beam wave type antenna is designed for large bandwidth operation tested between 3,6 and 6,4 GHz. The antenna and its composite feed were optimized to achieve the best possible parameters.

The antenna system cannot be modified with reasonable costs. It is likely that any modification will degrade the antenna merit factor so it is advisable to use it as built.

The tests performed on the composite feed-antenna assembly, at 5,840GHz, show a very good Voltage Standing Wave Ratio (VSWR) of 1,02.

The frequency sub-band allocated by ITU, to Radiolocation services in Region 1, within the C radar band, as described in *Radio Regulations, Edition 2012* is 5,250-5,850 GHz.

The best usable 20MHz band based on the antenna specified frequency range and the antenna feed waveguides is 5,830-5,850 GHz (partly overlapping the current 5,845 – 6,425 GHz antenna transmit band).

### 2.4 Antenna positioning/slewing speed limit

The actual antenna positioning/slewing speed is 0,3°/s on each axis.

An upgrade or a redesigning of the positioning system is needed in order to replace the technically obsolete existing system and, possibly, increase the tracking speed.

If the resulting precise tracking speed will be comparable with the actual rough slewing speed, low LEOs will still be reliably tracked but only at low elevations (i.e. 20° for 200 km altitude LEOs).

### 2.5 Antenna beamwidth limitation

The antenna beamwidth in the C-band is 0,11°.

This limits the angular resolution to 0,06° if no monopulse solution is used and, combined with the limited antenna positioning and slewing speed, makes the radar suitable mostly for space tracking missions.

### 2.6 Antenna steering domain limitation

Each antenna is partially steerable in an azimuth-and-elevation mount. The mechanical system configurations for the azimuth axis are,  $\pm 170^{\circ}$  around South in azimuth (“dead sector”  $\pm 10^{\circ}$  around North) and  $0^{\circ}$  to  $92^{\circ}$  for the elevation axis.

This existing design imposes limitations in the sky coverage and tracking speed limits. In order eliminate the azimuth limitations, a modification of the cable twister is required. It may consist in a connection box and extension spiral mounted cables and in a

repositioning of the position stop sensors. The antenna positioning system should be redesigned for greater angular speed or at least be upgraded (motors, angular transducers, electronic control system) to eliminate the  $\pm 10^\circ$  around North azimuth limitation.

### 2.7 Other possible services

To observe most of the space objects without affecting the existing services, the site's antennas have to point south. Furthermore, in order to make bi-static or multi-static observations with other reception sites, the antennas have to point south-west.

## 3. TRACKING RADAR DESIGN

### 3.1 Design assumptions

The design of the retrofit was performed based on the following assumptions:

**Quasi-monostatic architecture:** in this architecture, both Cheia 1 and Cheia 2 antennas will be used. The analysis performed showed that this architecture is the only viable solution, taking into account the level of the received signals.

**C-band operation:** the antenna bandwidth allows to select either S-band or C-band but the C-band parameters are superior. The considered frequency range is 5830–5850 MHz. This is the closest range

to the current 5845–6425 MHz antenna transmit band, partly overlapping it.

**Dual Mode operation:** the CW mode offers better performances and is considered as a basic mode, but the pulsed (FH-P) mode could offer better performances in a dense target environment.

**Transmitted power:** for the amplifiers transmission power has been selected the value of 2,5 kW, which has shown to be the best tradeoff between costs and performance. An increase to 5 kW is also possible.

**Speed increase and monopulse tracking** of the antenna positioning system: the radar is able to offer good performance utilizing the existing motors and tracking system. These additional features can be implemented in the future replacing the existing components.

### 3.2 Radar General Diagram

The general diagram considered for the radar is presented in Fig. 2. The radar is designed as a very flexible structure, able to use both continuous wave (CW) signals and Frequency Hopping Pulsed (FH-P) signals. Its architecture is intended to transfer maximum functionality in the digital domain.

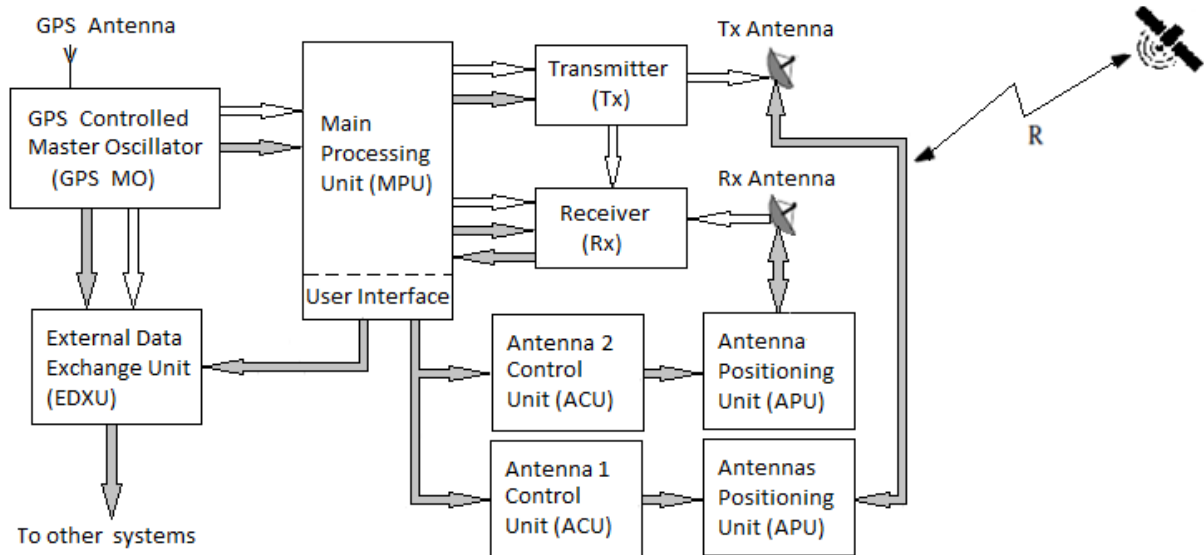


Figure 2. Radar general diagram

The diagram implements a high flexibility processing algorithm. The probing signals are generated by the **Transmitter**, based on the data received from the **Main processing unit (MPU)**. The generated signals are amplified to the required level (2,5 kW) by the linear High Power Amplifier that is part of the **Transmitter** and then applied to the Left Hand Circular Polarization (LHCP) port of the **Transmission (Tx) Antenna**.

The echo signals are received at the Right Hand Circular Polarization (RHCP) port of the **Reception (Rx) Antenna**, filtered, frequency translated and amplified into the **Receiver** to the level required by an optimal operation of the Analog-Digital Converter that is part of the receiver. The digital signal is translated into the frequency domain and sent as data to the **Main processing unit**.

The **Main processing unit** is a high computational power system that controls the radar operation through algorithm based commands grouped into three subsystems. The first group applies processing algorithms on received data, extracting targets and their parameters. The second group is deciding on the type and parameters of the probing signal that is going to be generated by the **Transmitter**, based on the operator's request or on operational criteria such as orbital height, size of the target, required precision, etc. The third group is deciding on the antennas positioning based on the actual position, on the target parameters and on existing orbital data.

The operator selected target data is sent to other external systems by the **External Data Exchange Unit** through VPNs. The external system might be an additional processing facility, a secure storing facility or other ESA member state facility. The **External data exchange unit** is responsible of managing the secure access to generated data (through user/password pair, token or any authentication method) and to requests and data from other entities. To ensure the system resolution, all blocks are synchronized by a GPS controlled high stability Master Oscillator (GPS MO).

The Tx and Rx antennas movement and position is controlled by the two Antenna Positioning Systems (APS) composed of the **Antennas Control Unit (ACU)** and the **Antennas Positioning Unit (APU)**. The APS are controlled by the **MPU** in order to provide

simultaneous movement of the Tx and Rx antennas so that they point simultaneously towards the target with the high precision required by tracking.

The radar will operate in 4 range scales, software selectable by the operator or by the tracking algorithm. It is to be noted that each scale limits are software imposed, the real scale limits being at least 5% larger, in order to avoid losing the target when switching between scales.

## 4. ESTIMATED PERFORMANCES

### 4.1 Amount and size of detectable objects

The estimation of the number of objects expected to pass through the antenna field of regard, and subsequently to be detectable and trackable by the radar was made using the ESA's "PROOF-2009" software, as a basic simulation tool, and the subsequent post-processing was made using spreadsheet applications. Since PROOF-2009 is designed for low duty cycle pulsed radars, the parameters of the proposed CW or high duty cycle pulsed radar were mapped to parameters of the equivalent low-duty cycle radar in terms of detection capabilities.

The simulation was based on the ESA "MASTER-2009" objects files, containing a list of known space debris, by setting "PROOF-2009" analysis mode to "Statistical" and inserting the specific parameters of the Cheia geographic coordinates and the radar parameters required. The starting time of the simulations was set to 2018.03.30 09:00 UTC, and the interval was set to 24 h.

The minimum detectable object size according to the orbital altitude in the CW mode is presented in Fig. 3.

The results of the PROOF-2009 simulation, showing the amount of detectable objects, per day, at different elevations, in the CW mode, are presented in Fig. 4.

The minimum detectable object size according to the orbital altitude in the FH-P mode is presented in Fig. 5.

The results of the PROOF-2009 simulation, showing the amount of detectable objects, per day, at different elevations, in the FH-P mode, are presented in Fig. 6.

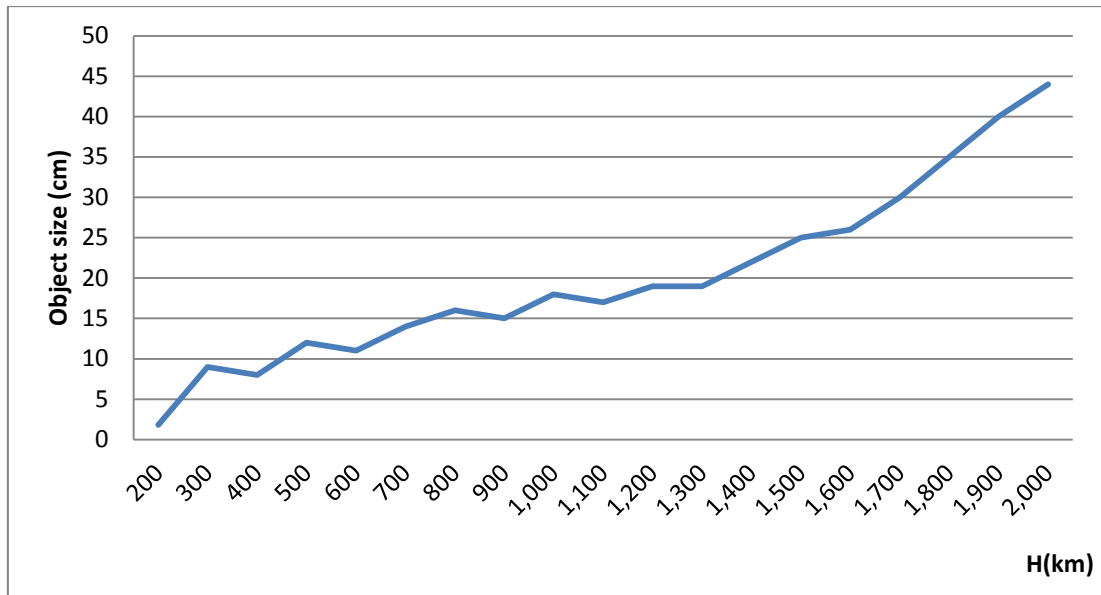


Figure 3. Minimum size of detectable objects in CW mode

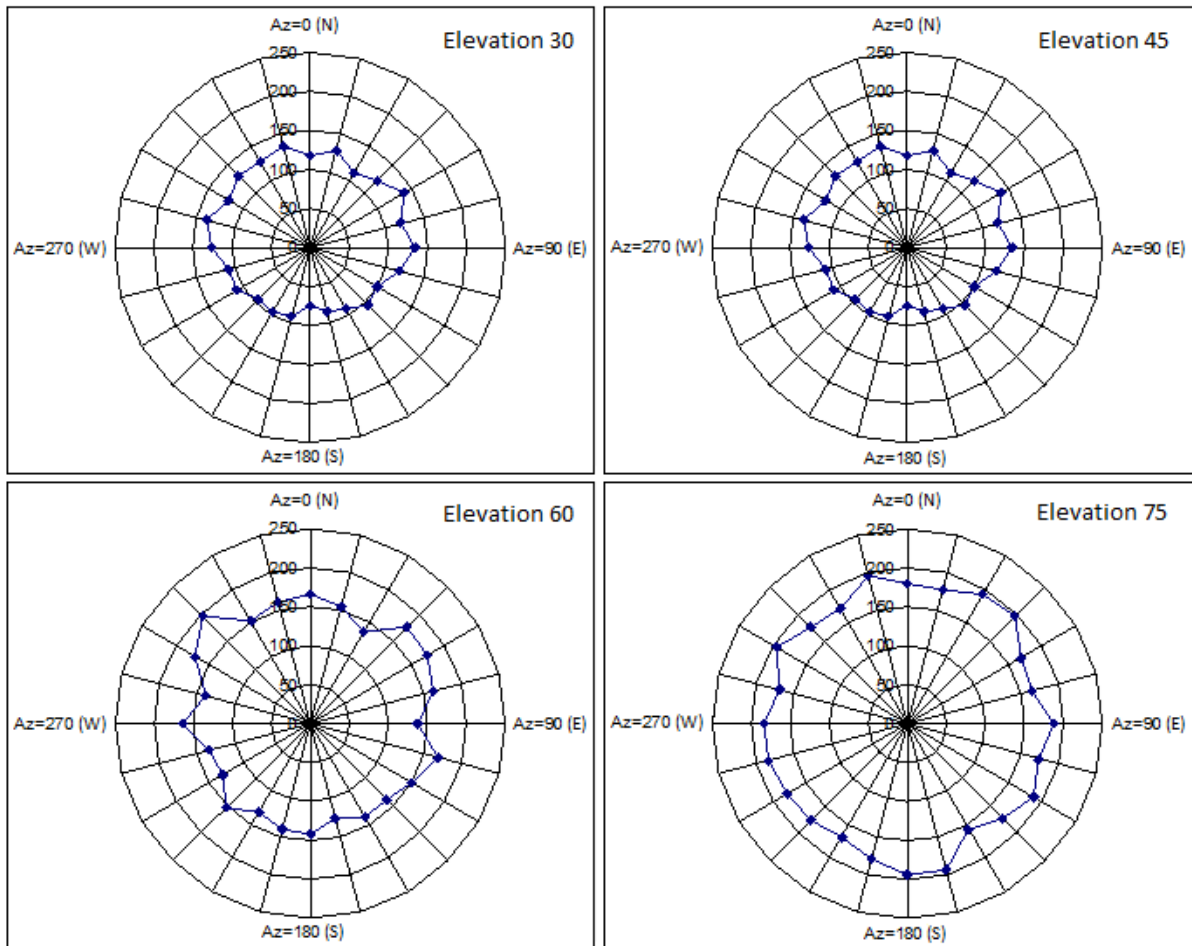


Figure 4. Amount of objects trackable by the radar at different elevations in CW mode

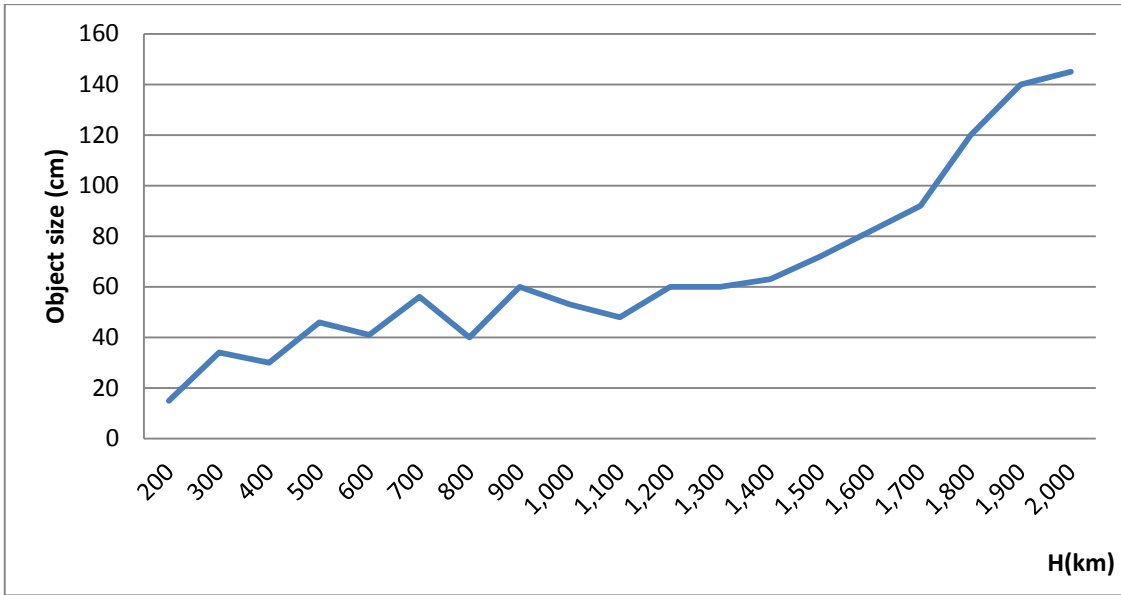


Figure 5. Minimum size of detectable objects in FH-P mode

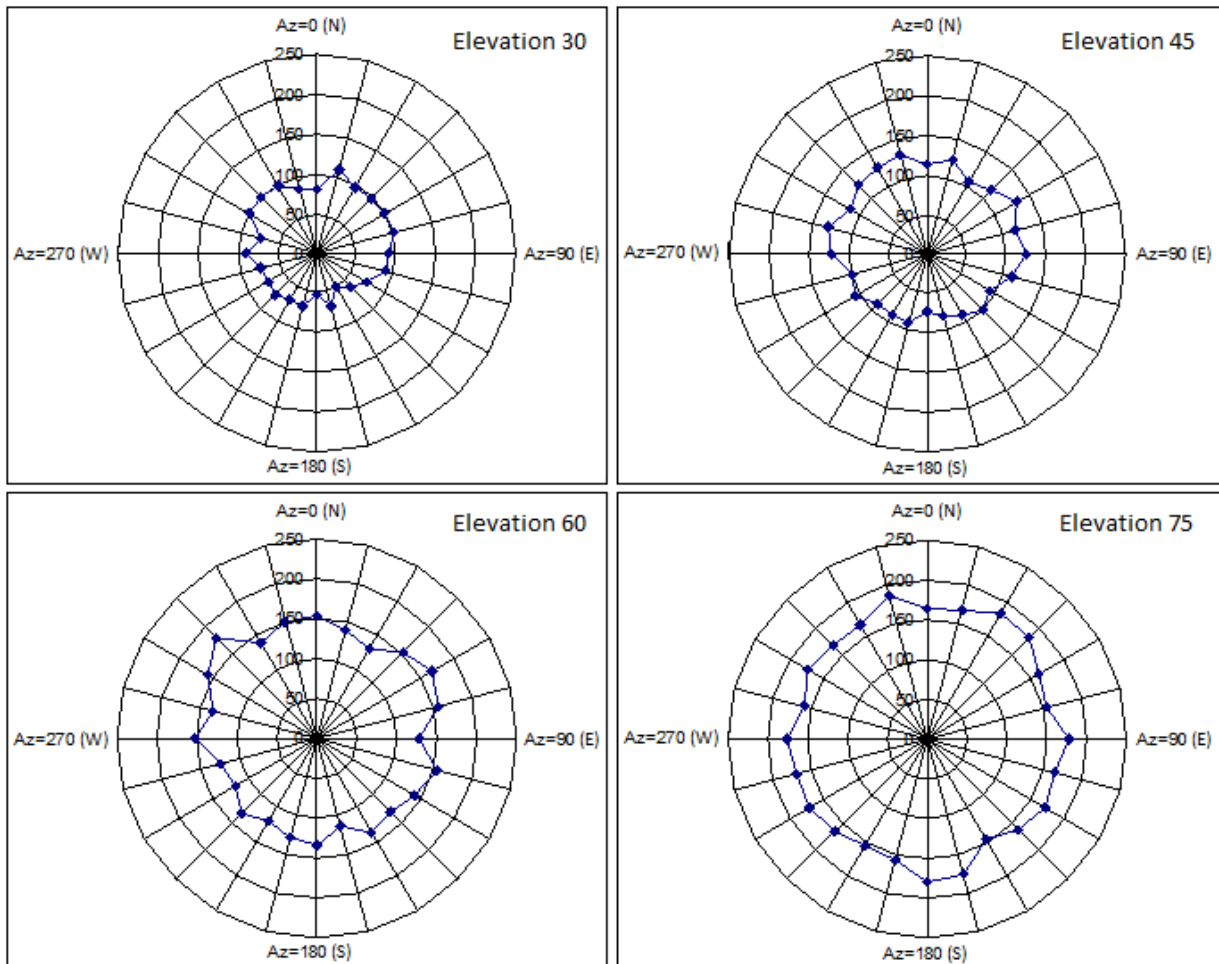


Figure 6. Amount of objects trackable by the radar at different elevations in FH-P mode

#### 4.2 Average observed track duration

The overall number of objects passing possible to be tracked with actual antenna speed parameters is 47068 per day, which represents more than 98,16% of the number of objects passing above  $20^{\circ}$  (the minimum unobstructed elevation limit) and in the range between 200 km and 5900 km at Cheia location. The starting time of the simulations was set to 2018.03.30 09:00 UTC, and the interval was set to 24 h.

Fig. 5 shows the histogram of the orbital regimes for the  $20^{\circ}$  minimum elevation limits and for all the passages. It can be seen that the number of passes in orbital regimes above 2000 km is very small, in fact is 1747, which represent less than 3.65% of the total number of passes.

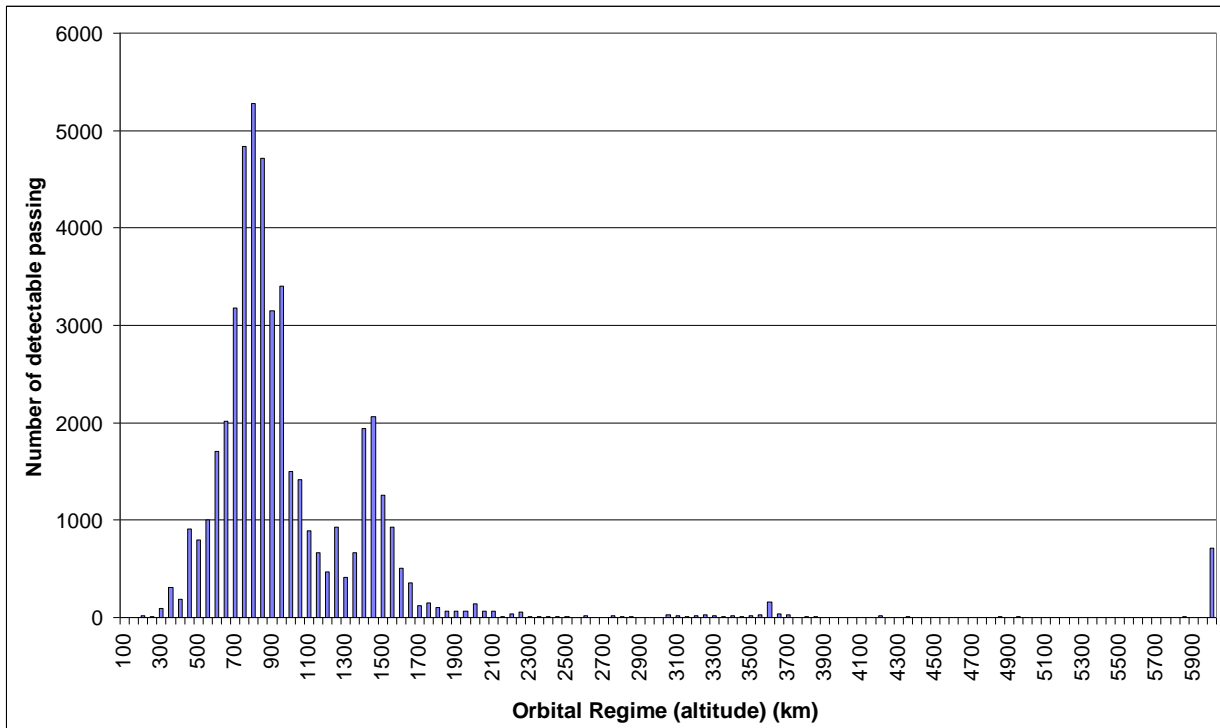


Figure 7. Histogram of the orbital regimes for the  $20^{\circ}$  lower limits elevation for all passes

To determine how often objects can be observed at certain altitudes, the mean, the standard deviation and the median for angular arc tracking and track time were computed. The results for orbital regimes up to 2000 km are illustrated in Fig. 7 to Fig. 14.

It should be noted that the tracking times (and angular arcs) are computed under the assumption of a straight circular cone antenna pattern, which for low elevation angles is not entirely correct. Due to the low positioning speed of the antenna, the low altitude targets (from 200 to 600 km) can be tracked only at low elevation angles ( $20^{\circ}$  to  $30^{\circ}$ ) where the target will move along the long axis of an ellipse, resulting from the intersection of antenna pattern (conical surface) with a skew plane. The apparent antenna beamwidth

(considering a plane perpendicular to the conical surface axis) for these cases is at least double ( $0,22^{\circ}$  at  $\epsilon=30^{\circ}$ ). As a result, the real tracking times and angular arcs are expected to be double.

The result presented in Fig. 7 correlated to those from Figs.12 to 14 shows that, from the total number of passing that cannot be tracked with the actual antenna speed parameters (881), the great majority (94,6 %) belong to the orbital regimes up to 750 km (834). The cumulative number of passing in orbital regimes up to 750 km is 10.238, which imply that less than 8,15 % of them cannot be tracked in these very low Earth orbital regimes.

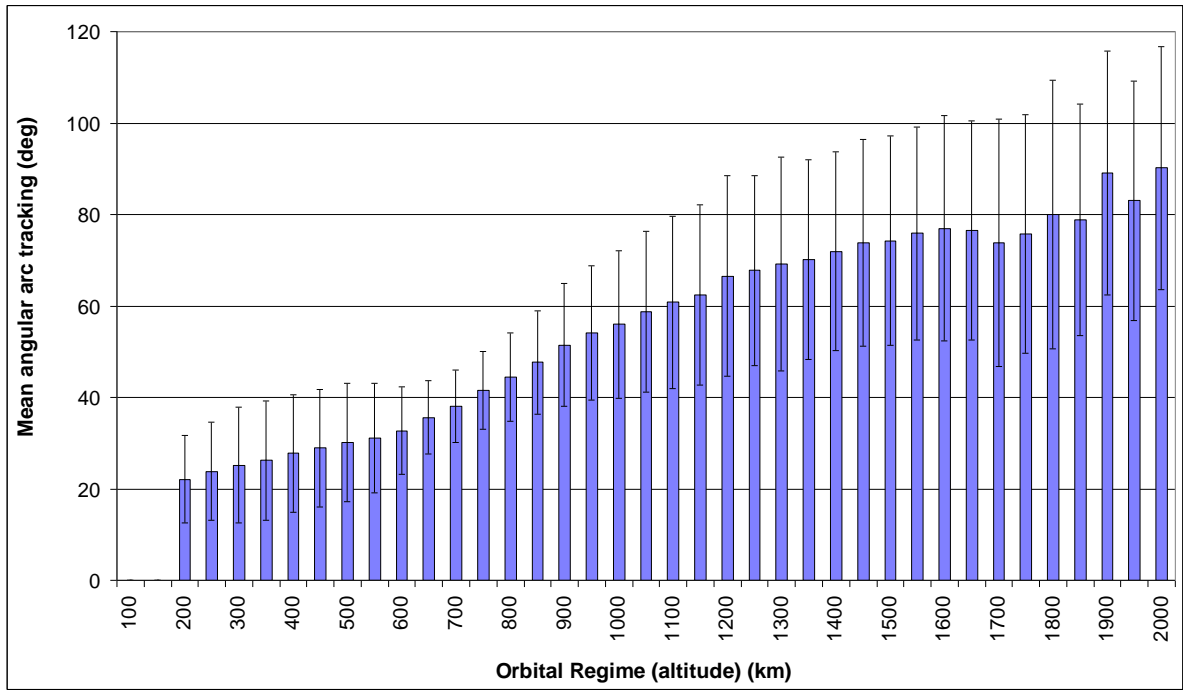


Figure 8. Mean angular arc tracking

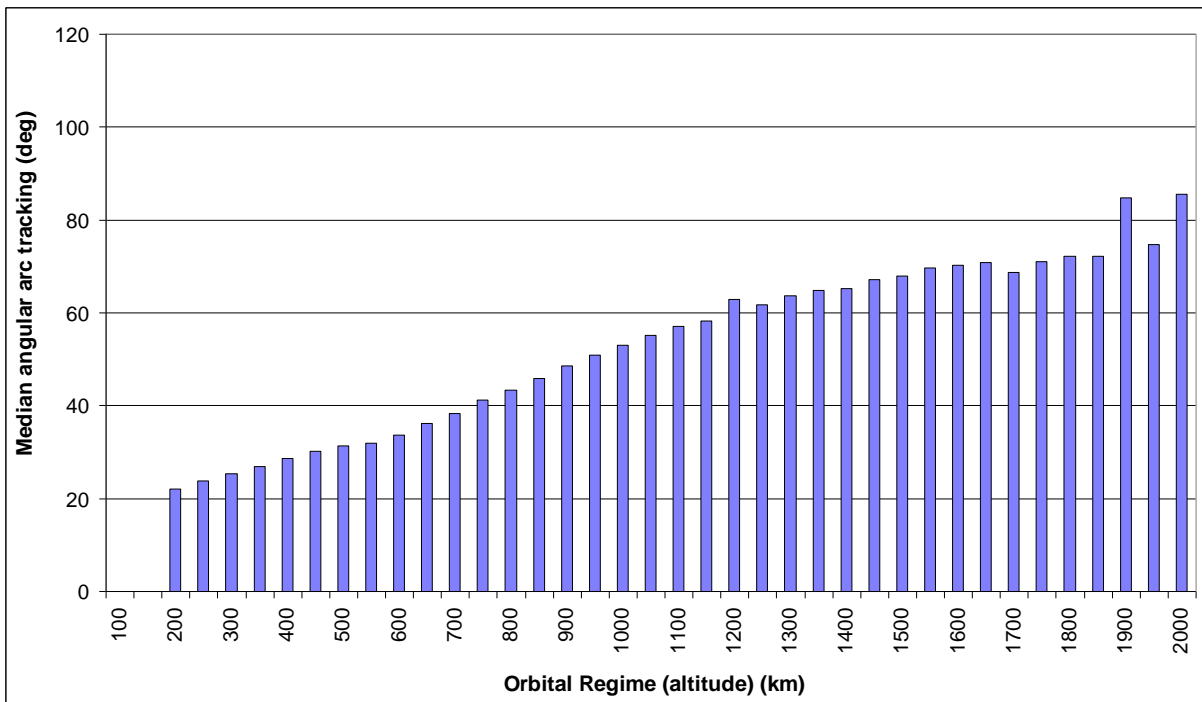


Figure 9. Median angular arc tracking



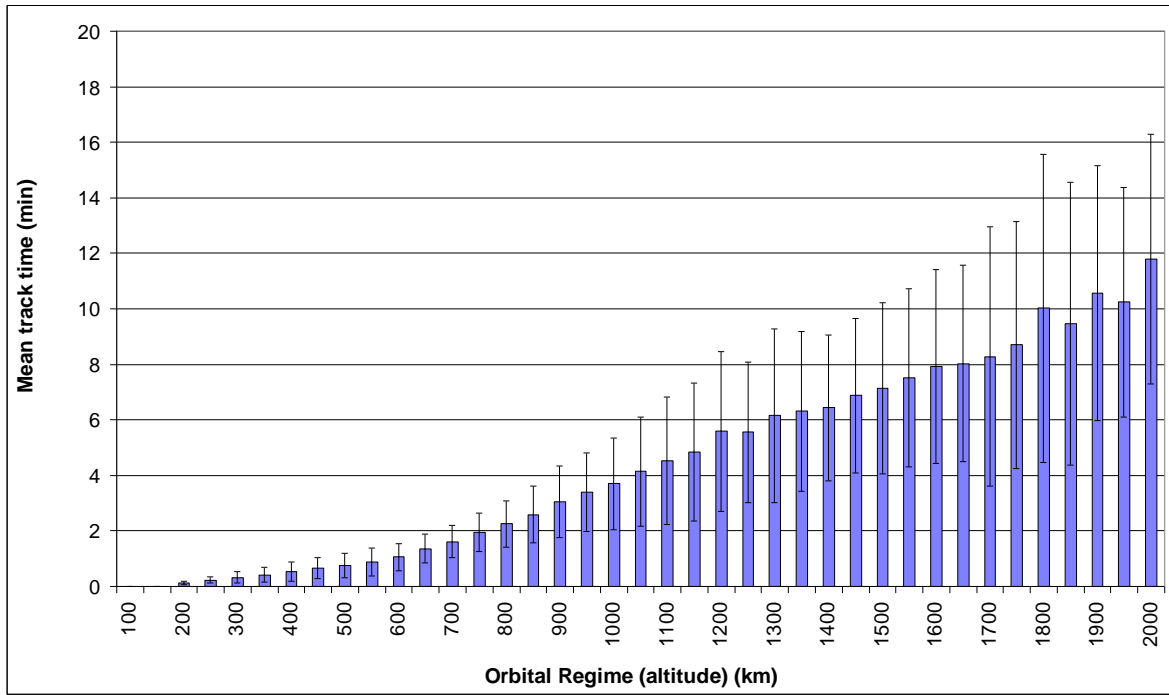


Figure 10. Mean track time

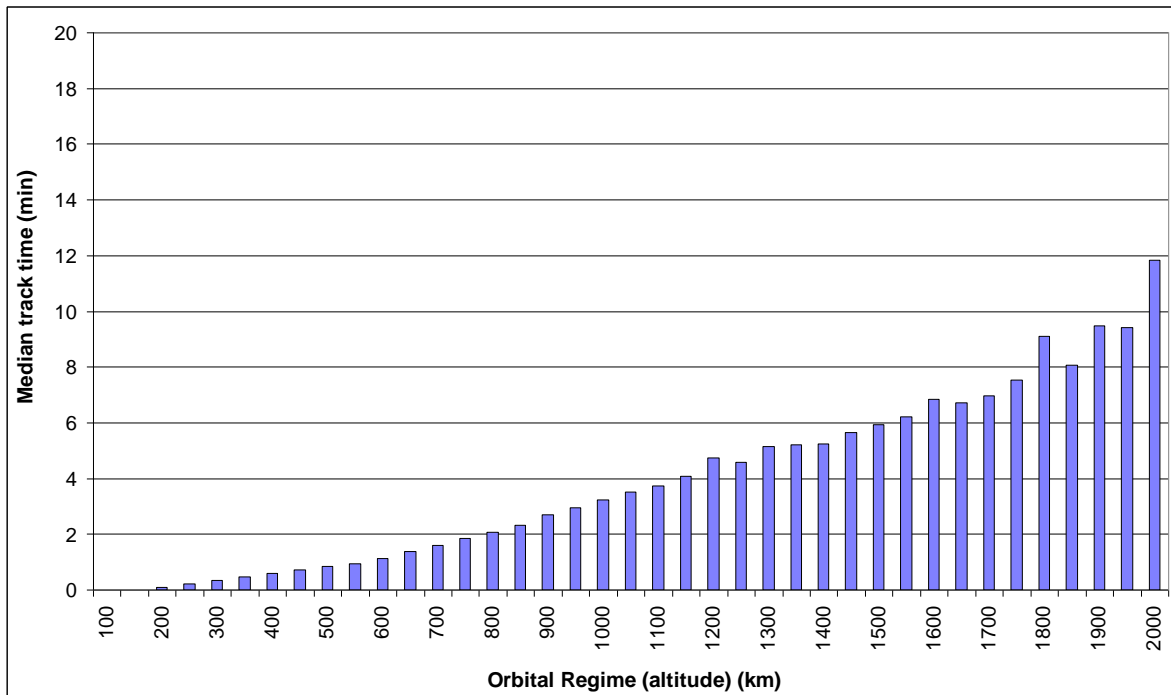


Figure 11. Median track time

There are three adjacent orbital regimes with the highest density of objects detectable (750 to 800 km, 800 to 850 km, and 850 to 900 km altitude above Earth). The total number of passes in the joint orbital

regimes (750 to 900km) is 14.836, representing 30,94% of the total number of passes. The corresponding number of detectable distinct satellites is 4.394 satellites (32% of the total number of detectable

satellites). For all these passes /objects the average time between tracks in the cases of satellites with

multiple passes in 24h interval is presented in Fig. 12, Fig. 13 and Fig. 14.

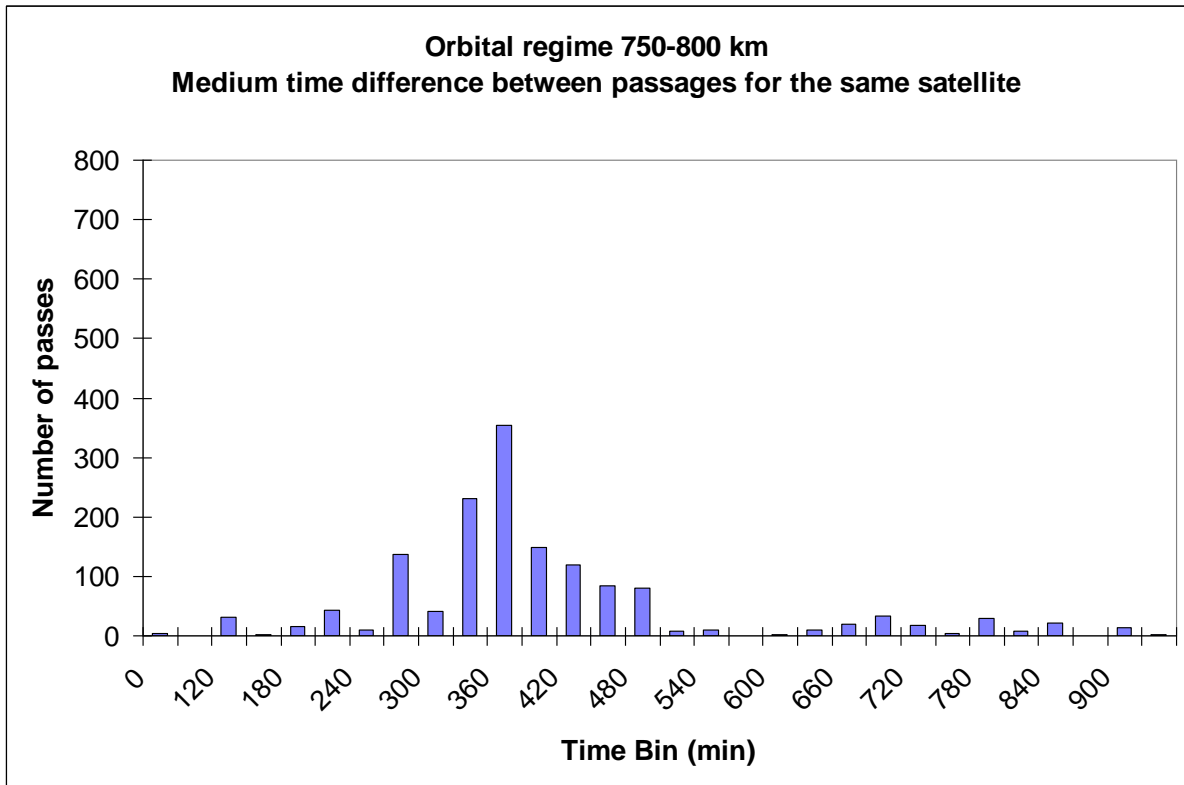


Figure 12. Number of passes per time bin 750-800 km orbital regime

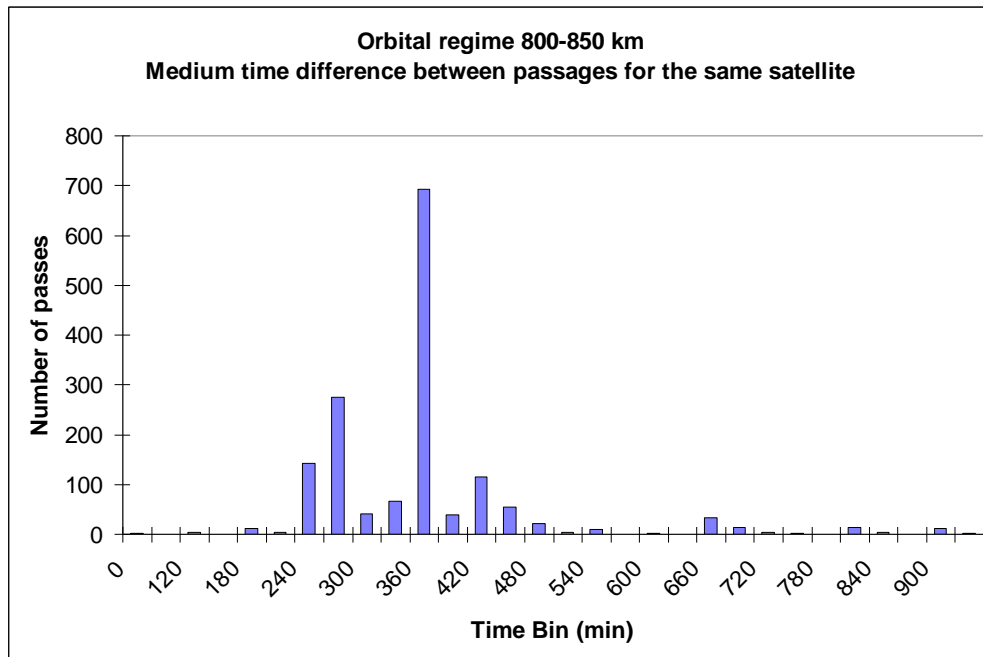


Figure 13. Number of passes per time bin 800-850 km orbital regime

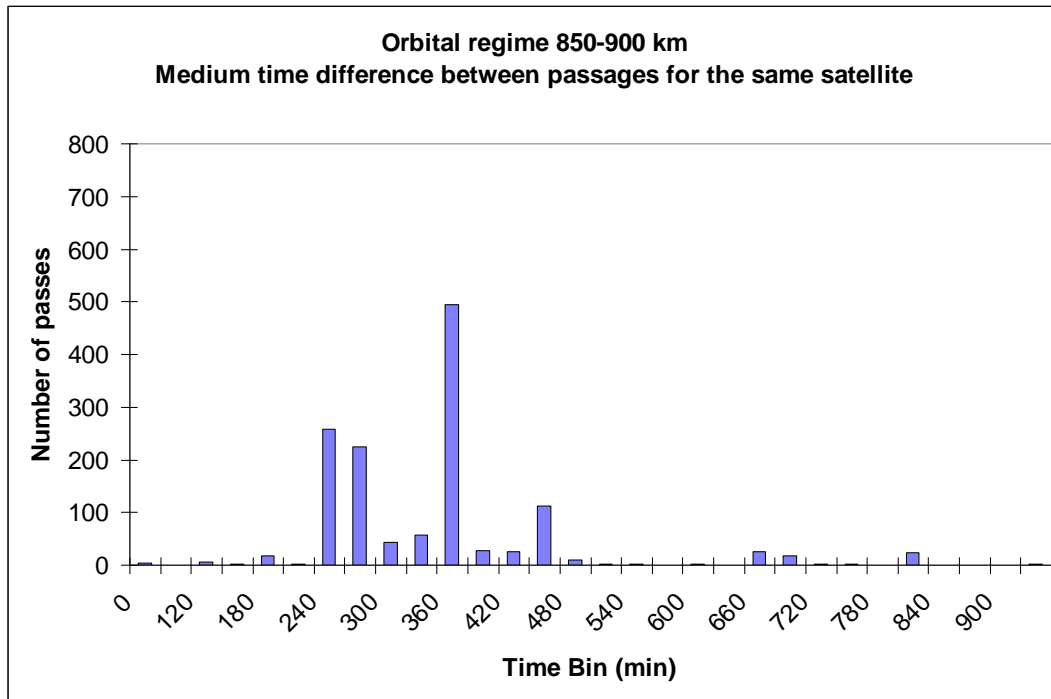


Figure 14. Number of passes per time bin 850-900 km orbital regime

The total number of the objects with two or more passing in 750 to 800km orbital regime is 1471, and 3 satellites with one passing. The average and median times per passing are: 1,95 min and 1,86 min.

The total number of the objects with two or more passing in 800 to 850km orbital regime is 1561, and only 1 satellite with one passing. The average and median times per passing are: 2,25 min and 2,08 min.

The total number of the objects with two or more passing in 850 to 900km orbital regime is 1355, and 3 satellites with one passing. The average and median times per passing are: 2,59 min and 2,32 min.

The simulations show that the radar will be able to repeatedly see the same object for a mean tracking period of at least 1,86 minute and at an average delay between tracks of at least 360 minutes, for the maximum number of objects in the time bin (355, 692, 495 in the three orbital regimes considered).

Based on the actual positioning speed of the antenna, it is estimated that the average time interval needed to point the antenna from the end of a track to the expected start position of the next scheduled track, is 4 to 6 minutes.

Consequently, the resulting time per satellite track is between 6 to 8 minutes (tracking time of the current

object, time to compute if the following object is trackable and positioning time needed for the next object) and the estimated numbers of trackable objects within the domain of orbital regimes between 750 km to 900 km, in 24 hours, is between 180 and 240. The maximum number of distinct objects observed in 2 passing in 24 hour is between 90 and 120.

## 5. CONCLUSIONS

The simulations show that Cheia SST radar will be capable to repeatedly track the same object for a mean tracking period of at least 1,86 minute, with an average period between tracks of at least 360 minutes for the same object. The resulting time per object is between 6 to 8 minutes (including the positioning time needed for the next object, estimated 4 to 6 min.). The time could be reduced by 30% if the antenna positioning speed is doubled.

The estimated number of objects trackable in 24 hours is between 180 and 240 (distinct objects tracked in 2 passages between 90 and 120). The number of tracked objects could be increased by 25% to 40% if the antenna positioning speed is doubled (optional).

The Quasi-monostatic architecture used for the radar design allows the use of Continuous Wave (CW LFM) or Pulsed (FH P-LFM) probing signals.

The radar is able to track LEOs at all altitudes, using the present antenna positioning speed. Low LEOs can however, be tracked only at low antenna elevation angles (20° for 200km altitude LEOs). Since the antenna positioning system has to be upgraded, it is advisable that the new antenna positioning system design makes provisions for the increase of the present speed, aiming to double it, if possible.

The total System availability is over 96%. An annual maintenance down time 2,5% (9 days/year), a foreseeable downtime due to helicopter flights over the site of 0,27% (1 day/year) and a possible 1,23% down time (4,5 days/year) due to adverse climate conditions (heavy snow, strong wind gusts, frozen rain) and other special situations are considered.

## REFERENCES

[1] Sven Flegel, Johannes Gelhaus, Marek Möckel, Carsten Wiedemann, Daniel Kempf, Consultants: Dr. Michael Oswald, Dr. Sebastian Stabroth, Cenk Alagöz, ESOC Study Manager: Dr. Holger Krag ESA/ESOC OPS-GR; ***“MASTER-2009. Software User Manual”***; European Space Agency (ESA), 2011

[2] Sven Flegel, Johannes Gelhaus, Marek Möckel, Carsten Wiedemann, Daniel Kempf, Consultants: Dr. Michael Oswald, Dr. Sebastian Stabroth, Cenk Alagöz, ESOC Study Manager: Dr. Holger Krag ESA/ESOC OPS-GR ***“Maintenance of the ESA MASTER Model. Final Report”***; European Space Agency (ESA), 2011

[3] Heiner Klinkrad; ***“Space Debris. Models and Risk Analysis”***; Praxis Publishing; Springer; 2006

[4] Donald R. Wehner, ***“High-Resolution Radar”***, Artech House Radar Library

[5] Bassem R. Mahafza, Ph.D., ***“Radar Systems Analysis and Design using MATLAB”***, Chapman & Hall/Crc, Boca Raton London New York Washington, D.C.

[6] Anneke Stofberg ***“IQ Reflected Power Canceller for an FMCW radar”***, Master of Engineering Thesis, Faculty of Electrical and Electronic Engineering at Stellenbosch University, March 2014